

RESEARCH PAPER

## Effects of MWCNT Nanoparticle Doping on Optical and Structural Behavior of Polyvinyl Alcohol

Ali Saad Sresih\*, Mohammed Hadi Shinen, Maan Abd-Alameer Salih

Department of physics, College of science, University of Babylon, Iraq

### ARTICLE INFO

**Article History:**

Received 19 April 2024

Accepted 26 June 2024

Published 01 July 2024

**Keywords:**

Morphology

MWCNTs

Nanocomposites

Optical

PVA

Spin coating

### ABSTRACT

For environmentally friendly applications, the impact of Multi walled Carbon nanotubes (MWCNTs) on the optical and structural characteristics of a polyvinyl alcohol (PVA) blend has been investigated in this work. PVA blends loaded with MWCNTs (0 to 3% weight per cent) were equipped using the spin coating method. These movies were then analyzed using a variety of methods. These film samples underwent AFM and UV-visible analysis. The surface morphology of thin films was investigated using the atomic force microscope (AFM) technique. The results unequivocally demonstrated the similarity of the created films. The concentration of (MWCNTs) enhanced the average grain diameter, roughness and Root Mean Square (RMS) value. When MWCNT content is raised to 3 weight per cent, the direct energy gap of the composite blends decreases from 4.181 to 4.167 eV, according to UV-visible analysis. We investigate the effects of MWCNT amounts on the optical properties of different mixes. This study advances the continuous development of Nano composites, particularly by improving the gas sensor's increased sensitivity.

### How to cite this article

Sresih A., Shinen M., Salih M. Effects of MWCNT Nanoparticle Doping on Optical and Structural Behavior of Polyvinyl Alcohol. J Nanostruct, 2024; 14(3):741-750. DOI: 10.22052/JNS.2024.03.005

### INTRODUCTION

The main objective in the development of composite materials is to produce materials with improved mechanical and physical qualities that aren't found in each of their components. This is because of their extraordinary capacity for mutation and perfection in these attributes, which has driven the world's current development of these compositions into an unending race because of the pressing demand for these unique and distant attributes on the original restricting [1,2]. It is only recently that the majority of polymers have been used to produce inexpensive products with simple functionality. However, because technology was developing so quickly, some industrially used materials had to be replaced with better ones. Consequently, in a number of applications involving high temperatures and pressures,

polymers have replaced iron and aluminium [3,4]. The potential of polymer composites to produce materials with qualities like excellent flexibility, cheap cost, and low-temperature manufacture is unsurpassed [5,6]. It is possible to classify the polymers as natural or industrial. Natural polymers include things like rubber, cellulose, proteins, and starches. Among the several synthetic polymers are poly(vinyl chloride), polypropylene, nylons, polyethene, polyvinyl alcohol, polyesters, polyacrylamide, and polycarbonate [7-9]. Small but mighty, the word "nano" has become increasingly popular in recent years and has the power to alter the course of history. Nanotechnology is one of the most significant scientific areas of our time because it integrates knowledge from physics, chemistry, biology, medicine, informatics, and engineering. Though yet in its infancy, this field of

\* Corresponding Author Email: sci875.ali.sresih@student.uobabylon.edu.iq



This work is licensed under the Creative Commons Attribution 4.0 International License.

To view a copy of this license, visit <http://creativecommons.org/licenses/by/4.0/>.

technology has a great deal of promise to provide essential breakthroughs with real-world uses. Tools and processes related to nanotechnology can be used to produce and control new nano and biomaterials as well as nano devices [10,11].

The polymer known as poly(vinyl alcohol) (PVA) is semicrystalline. Its qualities include a high charge storage capacity, superior mechanical and thermal stability, and high dielectric strength [12,13]. The unique qualities of carbon nanotubes (CNTs) include excellent charge transmission, high mechanical strength, and thermal stability. The host matrix's characteristics were significantly improved when a tiny quantity of CNTs were added to the polymer [14].

The principal objective of the current work is to examine the synergistic effect of MWCNT nanoparticles on the optical and structural (morphology) properties of PVA. The world has become more industrialized, especially in the area of electronics, and many electronic components require improvement to solve various problems with optoelectronic devices. These are crucial things to remember. The study aims to make new films that can be utilized for these purposes.

#### MATERIALS AND METHODS

Sigma-Aldrich provided the polyvinyl alcohol (PVA), which has a molecular weight 146000. The source of pure multi-wall carbon nanotubes (MWCNTs) was Nanothinx (Greece). CNTs are 90 per cent pristine, with an outer diameter of 10–30 nm and a length of 10–30 μm. After verifying the purity of each chemical, we melted one gram of each and discovered that the melting points were highly near.

To prepare the solution, 5g of the PVA was dissolved in 130 mL of dissolved in water, After this, the mixture is put on the magnetic mixer and stirred well to dissolve the substance. Then MWCNTs added is to a solution for the purpose of mixing different proportions (0.01, 0.02 and 0.03) % gm., PVA mixed with MWCNTs for 4 samples as shone also placed on the magnetic mixer and stir well to dissolve the material within 25 minutes for each sample. 25 ml of the solution was taken and placed on the sedimentation surface glass, after that the films were prepared by spin coating at 2000 revolutions per mint. Ultimately, the films were meticulously removed and preserved in a dust-free area in preparation for additional research.

In addition, to ensure the purity of the materials used, we melted 1 gm of each substance. The result was that the melting point for each substance was very close to the degree indicated in the information tape attached to each package.

Subsequently, studies were conducted to examine the optical characteristics and surface morphology of the thin Nano composite films.

Digital instruments (Inc. BY2000) are used to first capture Atomic Force Microscope (AFM) micrographs in order to observe the surface roughness and topography of deposited thin films. Common characteristics derived from AFM height pictures include grain size and root mean square (RMS) roughness for topographic mapping, there are three main approaches: touch, non-contact, and intermittent tapping or contact. An AFM's tip is its most important part because of its Nano scale radius of curvature. A micro-scale cantilever, to which the tip is attached, senses the Van der Waals interaction and additional forces acting on the tip and sample. A Shimadzu UV-vis 1800 double-beam spectrophotometer, It recorded the transmittance (T) and absorbance (A) spectra of the generated samples over the 200–1200 nm scanning wavelength range at room temperature. A sample of the same type of glass is also used as a reference to cancel out the effect of the glass where it is put in front of the falling rays and they fall perpendicularly on the sample. the computation of the films' absorption coefficients at various wavelengths using transmittance and reflectance data. The values of the transition, the absorption coefficient ( $\alpha$ ), the direct energy gap ( $E_g$ ), the extinction coefficient (K), the reflectance (R), and the refractive index (n) were determined based on the measured A. The produced composites [15–22] were computed using the following formulas:

$$\alpha = (2.303.A)/t \quad (1)$$

$$(\alpha hv) = B (hv - E_g)^r \quad (2)$$

$$k_o = \frac{\alpha \lambda}{4 \pi} \quad (3)$$

$$R = 1 - (T * e^A)^{1/2} \quad (4)$$

$$n = \left[ \frac{4R}{1 - R^2} - K^2 \right]^{1/2} + \frac{1 + R}{1 - R} \quad (5)$$

Where t, B, hv, and r stand for the thickness of

the film, incident photon energy, and an electronic transition type-related parameter, respectively.

In addition, the ratio of a material's absorbed light intensity ( $I_A$ ) to its incoming light intensity ( $I_0$ ) is known as absorption [23].

$$A = \frac{I_A}{I_0} \quad (6)$$

The transmittance of a film is determined by dividing its incident ray ( $I_0$ ) intensity by its transmitting ray ( $I_T$ ) intensity, as expressed in the following formula [24]:

$$T = \frac{I_T}{I_0} \quad (7)$$

### RESULTS AND DISCUSSION

The tests (AFM) of the Nano films for both

pure (PVA) and doped (MWCNTs) films made by spin coating demonstrated a consistent almost surface shape, as shown in Fig. 1. Where it is evident that the roughness rose as the doped ratio increased. The average grain diameter likewise indicates the same tendency that the root mean square (RMS) did as the doped ratio increased. Table 1 suggests an enhanced crystalline structure with a higher percentage of carbon nanotubes, leading to larger particles and rougher surfaces. Fig. 2 illustrates how, compared to the pure PVA film, its surface has more pits and pores and is less smooth. Fig. 3 shows the uneven surfaces, with numerous strewn and hump-shaped grains. On the PVA/MWCNTs mix surface, Additionally, brilliant granules of different sizes and shapes are embedded in a quasi-homogeneous nature.

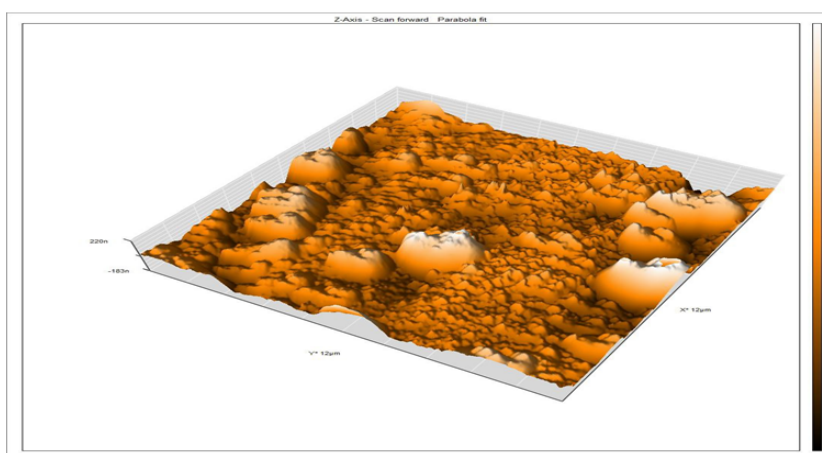


Fig. 1. 3D AFM images of pure thin PVA films.

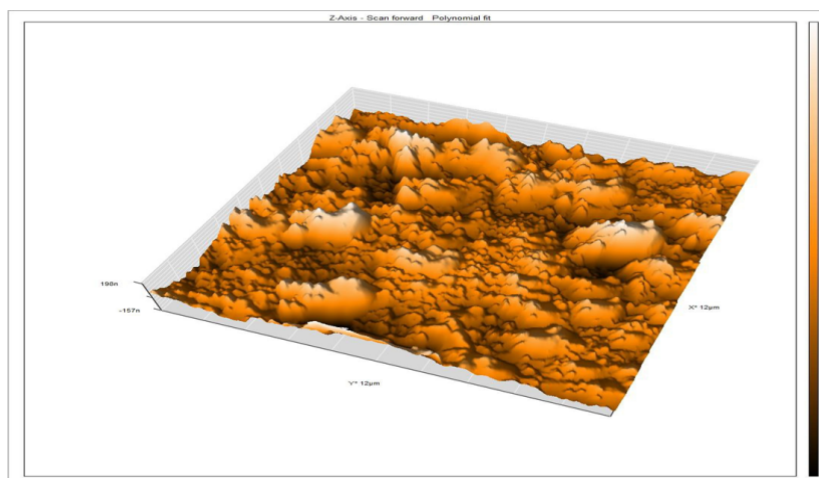


Fig. 2. 3D AFM pictures of a thin PVA sheet containing 1% MWCNTs.

MWCNTs are primarily responsible for these grains. As the MWCNT's weight percentage is raised to 3%, as seen in Fig. 4, the diameters of these agglomerations grow. Previous research documented similar traits [25,26].

It aims to characterize and study the optical properties of Nano composites (PVA-MWCNTs) Nano composite is to know the effect of doping multi wailed carbon nanotube nanoparticles on optical properties of PVA. This optical study includes the optical transmittance and absorption of Nano composites at room temperature, as well as calculating absorption, refractive and extinction

coefficients.

The chemical makeup, crystal structure, incident photon intensity, film thickness, and surface shape all affect optical absorption spectra. At ambient temperature, the absorption spectrum of thin PVA-MWCNTs sheet Nano composites with varied MWCNT concentrations was observed for the 285–400 nm wavelength range.

Fig. 5 demonstrates how the wavelength of the (PVA:MWCNTs) Nano composites affects the optical absorption. This spectrum indicates that all coatings exhibit more excellent UV absorption. After that, absorption reduces before it reaches

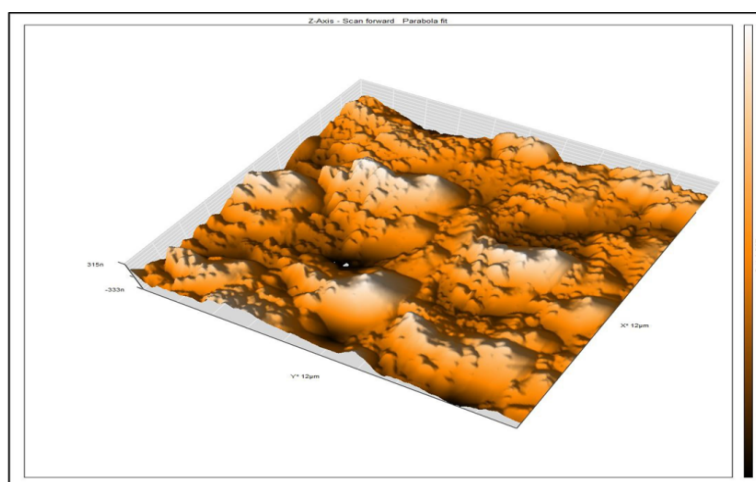


Fig. 3. 3D AFM scans of a thin film of PVA with 2% MWCNTs.

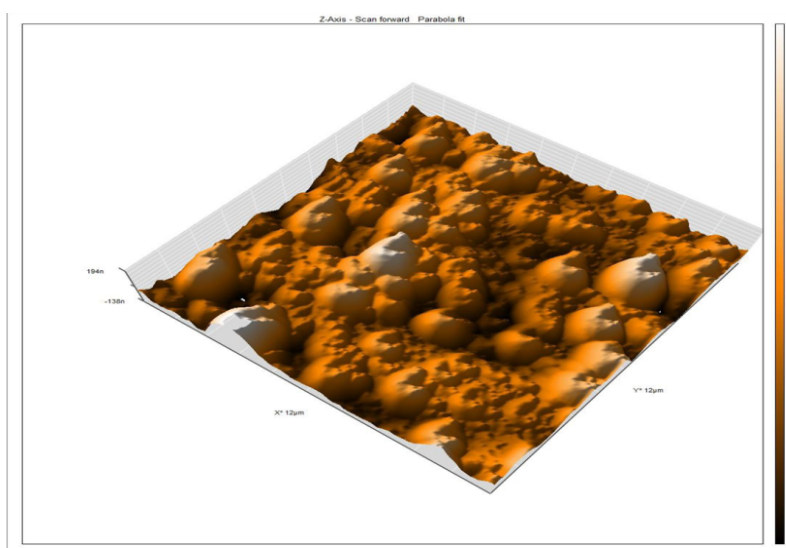


Fig. 4. 3D AFM photos of a thin film of PVA with 3% MWCNTs.

the visible spectrum because atoms cannot interact with the energy of the incident photons. The material absorbs the photon when it gets closer to the fundamental absorption edge due to interactions between the falling radiation and

the material beneath it. We find that when the weight ratios of the nanomaterial increase, the absorption decreases. This is the effect of free electrons absorbing incident light. This outcome agrees with the findings of the other researcher

Table 1. Morphological characteristics of thin PVA:MWCNTs film Nano films at different ratio.

| Sample          | Average grain diameter nm | Roughness nm | Root Mean Sq. nm |
|-----------------|---------------------------|--------------|------------------|
| PVA             | 46.23                     | 32.81        | 38.91            |
| PVA+ 0.01MWCNTs | 49.66                     | 4513         | 55.71            |
| PVA+ 0.02MWCNTs | 112.73                    | 60.68        | 78.64            |
| PVA+ 0.03MWCNTs | 119.53                    | 66.08        | 90.23            |

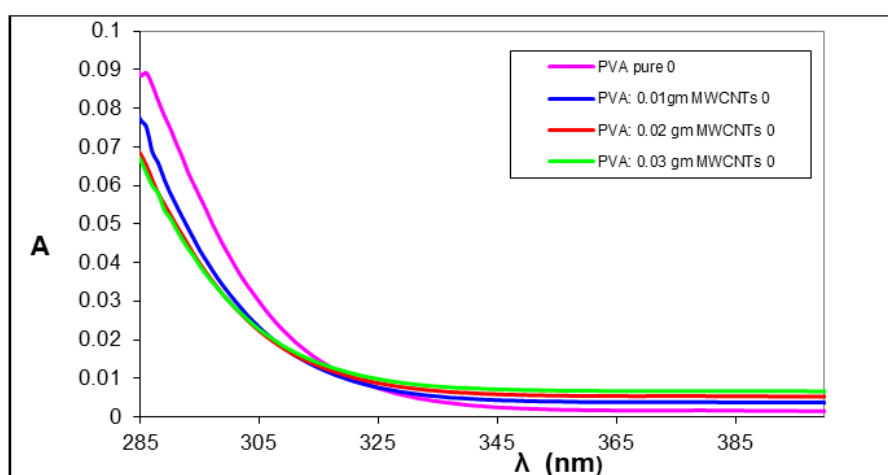


Fig. 5. Absorbance spectrum thin PVA:MWCNTs films.

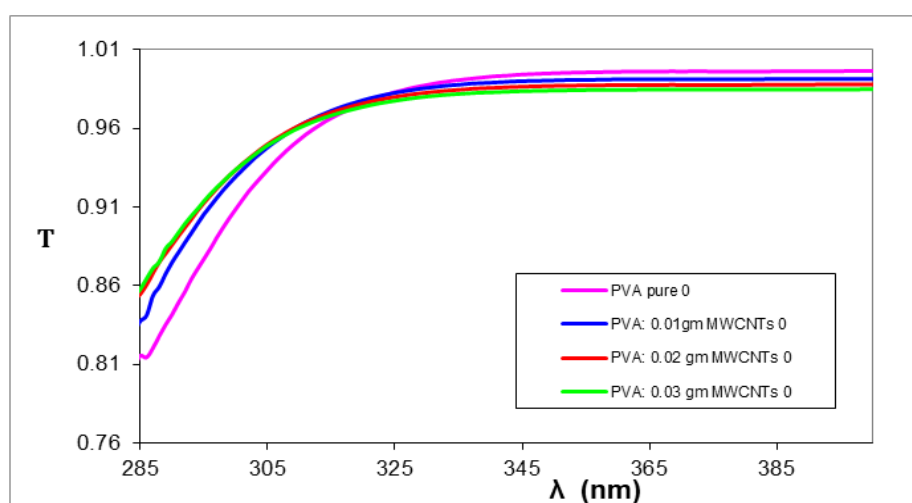


Fig. 6. PVA:MWCNTs thin-film transmittance spectrum as a function of wavelength.

[27]. Furthermore, at about 330 nm, a further absorption edge associated with the  $n \rightarrow \pi^*$  inter-band PVA transition is observed [17]. Compared to UV absorption at 285 nm, MWCNTs exhibit moderate absorption in the visible region [28].

Fig.6 shows that the transmittance for all samples increases with the increasing concentration MWCNTs nanoparticles and the reason for this rise is because the grains' crystal sizes have grown [29]. As for the higher transmittance in beginning the wavelength range of the spectrum High in the near Ultraviolet range at from (200-400 nm), this

is due to the absorption of light photons. Optical transmittance increases due to the regularity of the granular distribution, which is accompanied by a decrease in light scattering. This result agrees with the result of the other researcher [30].

Fig. 7 represents the relation between the reflectivity with wavelengths for pure PVA and doped with different ratio of MWCNTs. the incident photon with the variation of different thickness. With an increase in input photon wavelength across all films, the reflectance decreases quickly and reaches its maximum value at the wavelength

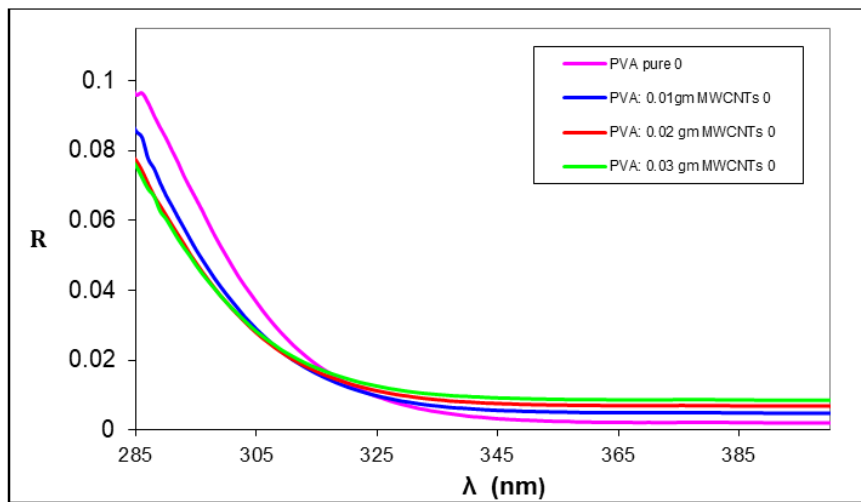


Fig. 7. The reflectance spectrum for PVA: MWCNTs thin films as a function of wave length.

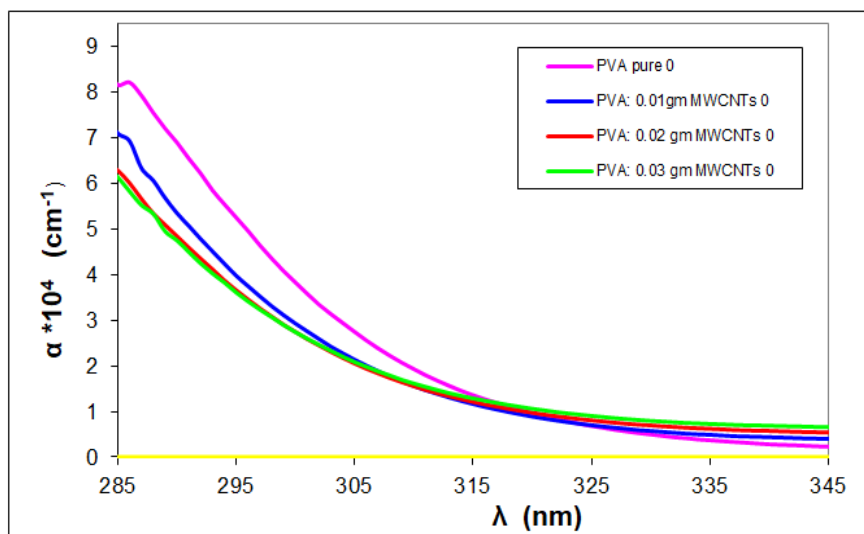


Fig. 8. Absorption coefficients for PVA: MWCNTs thin films as a function of wavelength.

of the film energy gap. This could function as a marker for the material absorption edge. These results are in agreement with reference [30].

All thin film values ( $\alpha$ ) are more than  $10^4 \text{ cm}^{-1}$  in the ultraviolet region. Fig. 8 illustrates how the absorption coefficient values of pure polymer and its doping decrease as the doping ratio concentration increases. The image shows that the absorption coefficient and absorbance spectrum act similarly. This is because of how they are related, as shown in equation 1.

Using the formula  $n = C / v$ , we may determine

the refractive index  $n$  at the speed of light in a vacuum instead of its speed in a substance. The morphological structure and the type of material have an impact on the  $n$  [31]. Fig. 9 shows that with the beginning the wavelength the refractive index will for the sample pure PVA Larger than other membranes, the uniform dispersion appears when the curve begins to decline 'and this is due to the decrease in absorption. We can see from this figure that when the concentration of nanoparticle weight percentages (MWCNTs) in polymer increases, the refractive index values fall. As

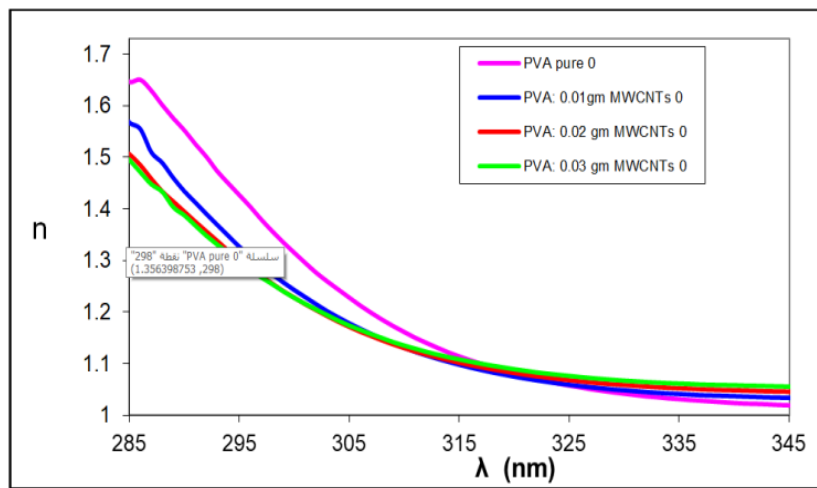


Fig. 9. The refraction index of PVA: MWCNTs.

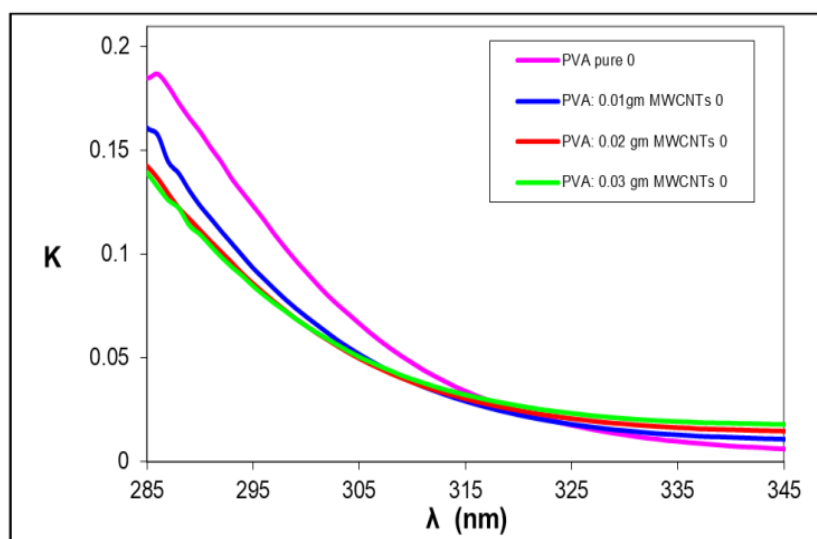


Fig. 10. Extinction coefficient of thin PVA: MWCNTs film.

MWCNTs was loaded alone with PVA, The shape of the refraction index curve for different parameters is similar to the reflectivity curve because the reflectance is associated with refraction index according to the same relationship. This result agrees with the result of the other researcher [32].

The attenuation of an electromagnetic wave travelling through a material is indicated by the extinction coefficient ( $K_o$ ), which measures the absorption energy in the thin film material. The density of free electrons in the material and structural flaws affect the values of ( $K_o$ ). Fig. 10 illustrates the correlation between the wavelength and extinction coefficient of PVA and PVA: MWCNTs thin films deposited. For all prepared

samples, it is generally evident that the extinction coefficient ( $K_o$ ) changes as the wavelength ( $\lambda$ ) increases. The extinction coefficient ( $K_o$ ) falls for every prepared sample as the number of MWCNTs increases. Generally speaking, the behaviour of ( $K_o$ ) is comparable to that of  $\alpha$ . These outcomes concur with reference [33].

Energy gaps have been calculated using equation (2) for the allowed and banned indirect transition band. Specifically, the predicted indirect transition band optical energy gap is allowed when  $r = 2$ , but it is prohibited when  $r = 3$ . Fig. 11 shows the relationship between the absorption edge  $(\alpha h\nu)^{1/2}$  for PVA and PVA. One may determine the energy gap for the indirect transition in MWCNTs

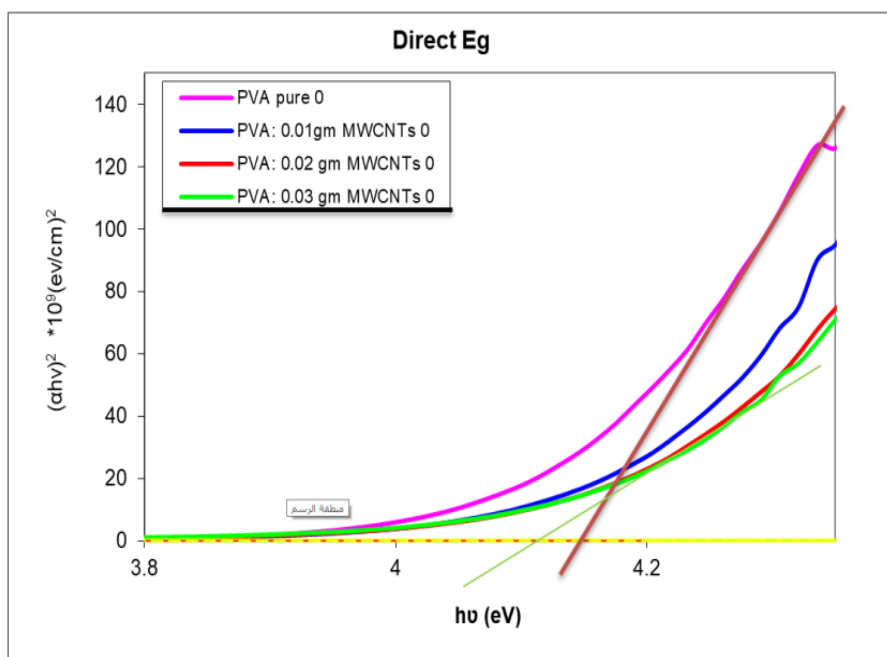


Fig. 11. Energy gap of thin PVA: MWCNTs films.

Table 2. The values of optical energy gap for forbidden direct transition for

| PVA/MWCNTs<br>gm | $E_g$ (eV)<br>forbidden |
|------------------|-------------------------|
| PVA pure         | 4.181                   |
| 0.01             | 4.175                   |
| 0.02             | 4.171                   |
| 0.03             | 4.167                   |



thin films by drawing a straight line at the value of  $(\alpha h\nu)^{1/2} = 0$  from the upper section of the curve towards the (x) axis. The resulting values are shown in Table 2. The optical energy gap values decrease as the weight percentages rise. In this case, the transition happens in two phases, with the electrons going from the valence band to the local levels and subsequently to the conduction band as a result of the weight % being increased. This is explained by the production of site levels in the forbidden optical energy gap. The heterogeneity of films that is, the fact that electrical conduction depends on additional concentration explains this phenomenon. The decrease in the direct energy gap can be explained by creating electronic pathways in the polymer, which enable electrons to go from the valence band to the conduction band when the weight proportion of PVA and PVA: MWCNTs increases. The findings of the second researcher support this assertion [34].

The primary cause of this fluctuation in (4.181 to 4.167 eV) is the expansion of the generated energy states between the HOMO and LUMO levels of the host blend's energetic band gaps. Additional variables leading to the decrease in the value are the increased density of voids, disorder, and flaws in the composite mixes due to the filling procedure [35].

## CONCLUSION

The following conclusions can be drawn from the PVA that was examined and doped with MWCNTs manufactured using the spin coating technique: The surface morphology of thin films was investigated using the atomic force microscope (AFM) technique. The findings showed that as the concentration of MWCNTs grew, the prepared average roughness, root mean square (RMS) values, and average grain diameter all increased. The inclusion of CNTs improved the qualities of PVA. When compared to absorption in the UV area at 265 nm, MWCNTs exhibit considerable absorption in the visible range. Moreover, noteworthy outcomes were observed about the decrease in absorbance with a rise in filler content, the increase in transmittance with an increase in MWCNTs, and the increase in reflection decrease with doping. The absorption coefficient, extinction coefficient, and refractive index all decrease with an increase in MWCNT content. Multi-wall carbon nanotubes (MWCNTs) and polymer (PVA) have the characteristics that make them the best choices

for gas sensors.

## CONFLICT OF INTEREST

The authors declare that there is no conflict of interests regarding the publication of this manuscript.

## REFERENCES

1. Abdali K. Structural, Morphological, and Gamma Ray Shielding (GRS) Characterization of HVCMC/PVP/PEG Polymer Blend Encapsulated with Silicon Dioxide Nanoparticles. *Silicon*. 2022;14(14):9111-9116.
2. Balazs AC, Emrick T, Russell TP. Nanoparticle Polymer Composites: Where Two Small Worlds Meet. *Science*. 2006;314(5802):1107-1110.
3. Abdali K. Structural, optical, electrical properties, and relative humidity sensor application of PVA/Dextrin polymeric blend loaded with silicon dioxide nanoparticles. *Journal of Materials Science: Materials in Electronics*. 2022;33(23):18199-18208.
4. Daniel M-C, Astruc D. Gold Nanoparticles: Assembly, Supramolecular Chemistry, Quantum-Size-Related Properties, and Applications toward Biology, Catalysis, and Nanotechnology. *Chem Rev*. 2003;104(1):293-346.
5. Abdali K, Abass KH, Al-Bermany E, Al-robayyi EM, Kadim AM. Morphological, Optical, Electrical Characterizations and Anti- Escherichia coli Bacterial Efficiency (AECBE) of PVA/PAAm/PEO Polymer Blend Doped with Silver NPs. *Nano Biomed Eng*. 2022;14(2).
6. Abdelrazek EM, Abdelghany AM, Badr SI, Morsi MA. Structural, optical, morphological and thermal properties of PEO/PVP blend containing different concentrations of biosynthesized Au nanoparticles. *Journal of Materials Research and Technology*. 2018;7(4):419-431.
7. Abdelrazek EM, El Damrawi G, Elashmawi IS, El-Shahawy A. The influence of  $\gamma$ -irradiation on some physical properties of chlorophyll/PMMA films. *Appl Surf Sci*. 2010;256(9):2711-2718.
8. Eissa MF, Kaid MA, Kamel NA. The influence of low- and high-linear energy transfers on some physical properties of poly(methyl-methacrylate) samples. *J Appl Polym Sci*. 2012;125(5):3682-3687.
9. Frey MW. Electrospinning Cellulose and Cellulose Derivatives. *Polymer Reviews*. 2008;48(2):378-391.
10. AbdAli MR, Jasim A, Hindi NKK. Prevalence of Human Monkeypox virus. *JOURNAL OF UNIVERSITY OF BABYLON for Pure and Applied Sciences*. 2023;54-61.
11. Alhuthali A, El-Nahass MM, Atta AA, Abd El-Raheem MM, Elsabawy KM, Hassanien AM. Study of topological morphology and optical properties of SnO<sub>2</sub> thin films deposited by RF sputtering technique. *J Lumin*. 2015;158:165-171.
12. El-naggar AM, Heiba ZK, Kamal AM, Mohamed MB. Assessment of performance based on structure, dielectric and linear/nonlinear optical properties of PVA/CMC/PVP blends loaded with ZnS/Co. *Optical and Quantum Electronics*. 2023;55(6).
13. El-naggar AM, Heiba ZK, Kamal AM, Altowairqi Y, Mohamed MB. Impact of loading PVA/CMC/PVP blend with CdSO<sub>0.9</sub>MO<sub>0.1</sub> non-stoichiometrically doped by transition metals (M). *Opt Mater*. 2022;133:113085.

14. Alghunaim NS. Optimization and spectroscopic studies on carbon nanotubes/PVA nanocomposites. *Results in Physics*. 2016;6:456-460.
15. Atta AA, El-Nahass MM, Elsabay KM, Abd El-Raheem MM, Hassanien AM, Alhuthali A, et al. Optical characteristics of transparent samarium oxide thin films deposited by the radio-frequency sputtering technique. *Pramana*. 2016;87(5).
16. Mostafa NY, Badawi A, Ahmed SI. Influence of Cu and Ag doping on structure and optical properties of  $\text{In}_2\text{O}_3$  thin film prepared by spray pyrolysis. *Results in Physics*. 2018;10:126-131.
17. Bouzidi A, Omri K, Jilani W, Guerhazi H, Yahia IS. Influence of  $\text{TiO}_2$  Incorporation on the Microstructure, Optical, and Dielectric Properties of  $\text{TiO}_2$ /Epoxy Composites. *Journal of Inorganic and Organometallic Polymers and Materials*. 2017;28(3):1114-1126.
18. Abdullah OG, Aziz SB, Rasheed MA. Structural and optical characterization of PVA: $\text{KMnO}_4$  based solid polymer electrolyte. *Results in Physics*. 2016;6:1103-1108.
19. Badawi A, Al-Gurashi WO, Al-Baradi AM, Abdel-Wahab F. Photoacoustic spectroscopy as a non-destructive technique for optical properties measurements of nanostructures. *Optik*. 2020;201:163389.
20. Badawi A, Al Otaibi AH, Albaradi AM, Al-Hosiny N, Alomairy SE. Tailoring the energy band gap of alloyed  $\text{Pb}_{1-x}\text{Zn}_x\text{S}$  quantum dots for photovoltaic applications. *Journal of Materials Science: Materials in Electronics*. 2018;29(24):20914-20922.
21. Amorphous and Liquid Semiconductors. Springer US; 1974.
22. Badawi A, Althobaiti MG. Effect of Cu-doping on the structure, FT-IR and optical properties of Titania for environmental-friendly applications. *Ceram Int*. 2021;47(8):11777-11785.
23. Ahmad K, Mobin SM. Graphene oxide based planar heterojunction perovskite solar cell under ambient condition. *New J Chem*. 2017;41(23):14253-14258.
24. Balen R, da Costa WV, de Lara Andrade J, Piai JF, Muniz EC, Companhoni MV, et al. Structural, thermal, optical properties and cytotoxicity of PMMA/ZnO fibers and films: Potential application in tissue engineering. *Appl Surf Sci*. 2016;385:257-267.
25. Bkakri R, Chehata N, Ltaief A, Kusmartseva OE, Kusmartsev FV, Song M, Bouazizi A. Effects of the graphene content on the conversion efficiency of P3HT:Graphene based organic solar cells. *Journal of Physics and Chemistry of Solids*. 2015;85:206-211.
26. Bkakri R, Kusmartseva OE, Kusmartsev FV, Song M, Bouazizi A. Degree of phase separation effects on the charge transfer properties of P3HT:Graphene nanocomposites. *J Lumin*. 2015;161:264-270.
27. Farag OF, Abdel-Fattah E. Synthesis and characterization PVA/plasma-functionalized MWCNTs nanocomposites films. *Journal of Polymer Research*. 2023;30(5).
28. Dwivedi N, Dubey KC, Shukla RK. Structural and optical studies of multi-walled carbon nanotubes. *Materials Today: Proceedings*. 2020;29:872-875.
29. Chiellini E, Corti A, D'Antone S, Solaro R. Biodegradation of poly (vinyl alcohol) based materials. *Prog Polym Sci*. 2003;28(6):963-1014.
30. El-naggag AM, Alsaggaf A, Heiba ZK, Kamal AM, Aldhafiri AM, Fatehmulla A, Mohamed MB. Exploring the structural, optical and electrical characteristics of PVA/PANi blends. *Opt Mater*. 2023;139:113771.
31. Zhang H, Wu J, Zhai C, Du N, Ma X, Yang D. From ZnO nanorods to 3D hollow microhemispheres: solvothermal synthesis, photoluminescence and gas sensor properties. *Nanotechnology*. 2007;18(45):455604.
32. Ben Doudou B, Chiba I, Daoues HS. Optical and thermo-optical properties of polyvinyl alcohol/carbon nanotubes composites investigated by prism coupling technique. *Opt Mater*. 2022;131:112672.
33. Electronic Properties and Charge Density Transfer of  $\text{MoTe}_2$ . *AUSTRALIAN JOURNAL OF BASIC AND APPLIED SCIENCES*. 2018.
34. Mohammed RM. Effect of Antimony Oxide Nanoparticles on Structural, Optical and AC Electrical Properties of (PEO-PVA) Blend for Antibacterial Applications. *International Journal of Emerging Trends in Engineering Research*. 2020;8(8):4726-4738.
35. Badawi A, Mersal GAM, Shaltout AA, Boman J, Alsawat M, Amin MA. Exploring the structural and optical properties of FeS filled graphene/PVA blend for environmental-friendly applications. *Journal of Polymer Research*. 2021;28(7).